

# 1 Tesla Bench-top MRI of a Mouse Model of Colorectal Carcinoma Metastasis in the Liver: Comparison with 9.4 Tesla

Rajiv Ramasawmy<sup>\*1,2</sup>, Thomas Roberts<sup>\*1,3</sup>, Bernard Siow<sup>1</sup>, Sean Peter Johnson<sup>1,2</sup>, Jack Anthony Wells<sup>1</sup>, Alan Bainbridge<sup>4</sup>, Rosamund Barbara Pedley<sup>2</sup>, Mark Francis Lythgoe<sup>†1</sup>, and Simon Walker-Samuel<sup>†1</sup>

<sup>1</sup>Centre for Advanced Biomedical Imaging, University College London, London, Greater London, United Kingdom, <sup>2</sup>Cancer Institute, University College London, London, Greater London, United Kingdom, <sup>3</sup>Centre for Mathematics and Physics in the Life Sciences and Experimental Biology, University College London, London, Greater London, United Kingdom, <sup>4</sup>Department of Medical Physics, University College London, London, Greater London, United Kingdom

**INTRODUCTION:** Recently, low-field MR scanners, for pre-clinical imaging, have come to market<sup>1</sup>. These so-called ‘bench-top’ scanners are compact, do not require cryogen-cooling, have no stray field, and offer a potential cost-saving over higher field alternatives. However, signal-to-noise characteristics are potentially compromised in return for affordability and convenience. One potential area of application for this type of instrumentation is in the measurement of the growth of orthotopic tumour xenograft models in mice or rats. Unlike conventional subcutaneous xenograft models, which are implanted under the skin and their growth typically monitored by palpation and/or caliper measurement, orthotopic models are grown in the clinically relevant organ. Furthermore, the siting of tumours in organs such as the brain or liver allows straightforward characterisation with MRI, allowing tumour volumes to be accurately measured and the time points at which to commence therapy studies to be reliably defined. However, whether bench-top MRI scanners offer sufficient SNR to allow this type of application in practically useful scan times, has not been evaluated. The purpose of this pilot study was therefore to compare the performance of a 1T, benchtop MRI system with a 9.4 T magnet, for the assessment of tumour volume in a mouse model of colorectal liver metastasis.

**METHODS:** Due to the inherent difficulty in comparing data acquired at different field strengths, 1T and 9.4T scanners were treated as different imaging modalities, with 9.4T data providing a ‘gold standard’ for comparison. The rationale for sequence design was to acquire images with sufficient signal-to-noise ratio (SNR) and contrast-to-noise ratio (CNR) to allow tumour tissue to be discriminated from background liver within a practically useful imaging time (less than 30 minutes). However, image resolution was matched between systems. Finally,  $T_1$  and  $T_2$  data were acquired for both tumour and liver in order to optimise tumour/liver contrast in future measurements.

**Animal model:** The SW1222 colorectal carcinoma cell line was injected intrasplenically at a concentration of  $1 \times 10^6$  cells in 100  $\mu$ l in serum free media into n=3 MF1 nu/nu mice. Cells were allowed to wash through to the liver for 1 minute followed by splenectomy. Imaging was performed at 5 weeks following surgery.

**Agilent 9.4T VNMRS** (Agilent Technologies, CA, USA). *High Resolution Anatomical:* Respiratory-triggered, multi-slice Fast Spin Echo (FSEMS),  $192^2$  matrix, FOV 30 mm<sup>2</sup>, slice thickness 0.75 mm,  $k_0$  3, ETL 4, effective TE 19 ms, TR 2s, 2 averages, acquisition time 7 minutes.  *$T_1$  mapping:* Respiratory triggered, single-shot, single-slice, Gradient Echo (GE), centric ordered readout, 128 x 128 matrix, FOV 30 x 30 mm<sup>2</sup>, slice thickness 1 mm, 10 exponentially spaced TIs, TR 6s, TE 5.7 ms, Flip Angle 15°.  *$T_2$  mapping:* Respiratory-triggered, multi-slice, multi-echo Spin Echo (MEMS),  $128^2$ , FOV 30 x 30 mm<sup>2</sup>, slice thickness 1 mm, TR 630 ms, TE 8.3 ms, 8 echoes.

**Bruker 1.0T ICON** (Bruker BioSciences Corporation, Ettlingen, Germany). *High Resolution Anatomical:* Respiratory-triggered, multi-slice Spin Echo,  $192^2$  matrix, FOV 30 mm<sup>2</sup>, slice thickness 0.75 mm, ETL 1, effective TE 32 ms, TR 2.8s, 3 averages, acquisition time 26 minutes.  *$T_1$  mapping:* Respiratory triggered, multi-slice, Gradient Echo (FLASH),  $128^2$  matrix, FOV 30 mm<sup>2</sup>, slice thickness 1.5 mm, 3 slices, 7 exponentially spaced TIs, TR 3.5s, TE 6 ms, Flip Angle 30°.  *$T_2$  mapping:* Respiratory-triggered, multi-slice, multi-echo Spin Echo (RARE), RARE factor 2,  $128^2$ , FOV 30 mm<sup>2</sup>, slice thickness 0.75 mm, TR 630 ms, TE 20 ms, 5 echoes.

**Image Analysis:** Liver and tumour volumes were delineated by manual segmentation of the high resolution anatomical images. 3D anatomical representations were generated using Amira 5.4 (Visage Imaging, USA).  $T_1$  and  $T_2$  maps were generated across the regions of interest in MATLAB (MathWorks, USA) using pixel-wise 3 and 2 parameter curve fits, respectively. Signal-to-noise was estimated using the ratio of tumour tissue signal magnitude to the variance of Rayleigh-distributed background noise<sup>2</sup>. Optimal anatomical scan parameters were estimated by maximising contrast-to-noise (CNR) in Bloch simulations.

**RESULTS:** Following 5 weeks of growth, the mean tumour volume was measured to be 2122 ( $\pm$  1130 SEM) mm<sup>3</sup> from 9.4T data, and 2066 ( $\pm$  1363 SEM) mm<sup>3</sup> from 1T data. Mean liver volume was measured to be 1245 ( $\pm$  159 SEM) mm<sup>3</sup> from 9.4T data and 1081 ( $\pm$  211 SEM) mm<sup>3</sup> from 1T data. Bland-Altman analysis of all volumes measured showed good agreement between field strengths, with a mean difference of 109 ( $\pm$  427 SD) mm<sup>3</sup> (6% under-estimate of total volumes at 1T). The mean signal-to-noise ratio of tumour tissue was 20.1 at 9.4T and 7.5 at 1T; the ratio of signal in tumours to that of background tissue was 149% at 9.4T and 153% at 1T.  $T_1$  and  $T_2$  data are reported in Table 1. Mean  $T_1$  values in both tissues were approximately a factor of 4 lower at 1T; faster longitudinal relaxation is expected at lower field. Mean tumour and liver  $T_2$  values were a factor of 2-3 higher than at 1T, possibly reflecting both the different sequences used and diffusion effects causing faster dephasing at higher field strengths between multiple echoes. Optimisation was performed using the relaxivity measurements, from which it was deduced that optimal contrast between tumour and liver would be achieved using TR/TE = 3s/66ms at 1T, close to the parameter values used in this study.

**DISCUSSION:** Despite reductions in signal-to-noise at low field, we have shown that volumetric analysis of mouse liver tumours at 1T is comparable with those at 9.4T, and could be easily extended to quantifying the sizes of other organs. Anatomical resolution was maintained between fields although data at lower field strength took longer to acquire (26 minutes at 1T, compared with 7 minutes at 9.4T). The minimum tumour size detectable at both field strengths has yet to be determined.  $T_1$  and  $T_2$  values were also reported although direct quantitative comparison will require phantom reference scans at both field strengths to determine sequence dependence on relaxation times. Contrast between tumour and liver could potentially be improved with gadolinium-based contrast agents, which have greater relaxivity at lower field strengths<sup>3</sup>. This would also allow a shorter echo time to be used than the optimised value of 66ms deduced in this study, which would most likely suffer from prohibitively low SNR. To conclude, bench-top MRI offers promise for low-cost, accurate measurement of tumour volume in orthotopic tumour xenograft models.

**REFERENCES:** [1] A. Schmid et al. *Mol. Imaging Biol.* (2013), **15**:155-165. [2] S. Walker-Samuel et al. *Magn Reson Med* (2009), **62**:420-429. [3] P. Caravan et al. *Contrast Media Mol. Imaging* (2009), 4:89-100.

<sup>\*</sup>Joint First Authors <sup>†</sup>Joint Senior Authors

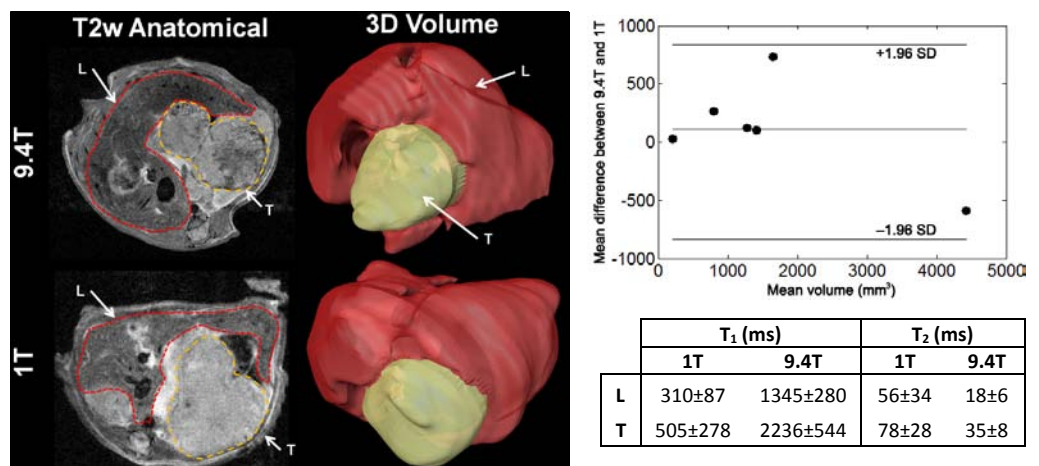


**Fig 1: Representative data, from the same animal, at 1 and 9.4T, showing  $T_2$ -weighted anatomical images with tumour (T) and liver (L) segmentation, and corresponding 3D volumetric visualisation. Fig 2: Bland-Altman comparison of all volumes with 95% confidence intervals. Table 1: Mean  $T_1$  and  $T_2$  values ( $\pm$  SEM) at 1T and 9.4T**